ORGANIC LETTERS

2013
Vol. 15, No. 7
1768–1771

Phenanthro[9,10-*d*]imidazole-quinoline Boron Difluoride Dyes with Solid-State Red Fluorescence

Weiling Li, Weiying Lin,* Jiaoliang Wang, and Xiaoyu Guan

State Key Laboratory of Chemo/Biosensing and Chemometrics, College of Chemistry and Chemical Engineering, Hunan University, Changsha, Hunan 410082, P. R. China

weiyinglin@hnu.edu.cn

Received March 6, 2013

ABSTRACT

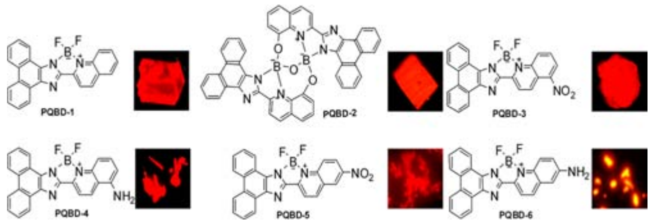

A new family of boron difluoride-rigidified dyes, phenanthro[9,10-*d*]imidazole-quinoline boron difluoride (PQBD), with solid-state fluorescence has been designed and synthesized. The novel series of PQBD are advantageous over the typical boron difluoride-rigidified dyes such as BODIPYs in terms of large Stokes shift and red fluorescence in the solid state.

Efficient solid-state fluorescent dyes are required in the fields of both fundamental research and optoelectronic materials. Thus, the development of solid-emissive fluorophores has attracted great attention.[1] A major hurdle faced in the design of solid-emissive dyes is to overcome fluorescence quenching in the solid state. Toward this end, several strategies including aggregation-induced emission[2] and incorporation of bulky groups[3] have been employed. However, it is still very challenging to rationally design new families of solid-emissive fluorophores, in particular, based on novel frameworks.

In this paper, we describe the design, synthesis, photophysical properties, and X-ray structural analysis of a series of phenanthro[9,10-*d*]imidazole-quinoline boron difluorides (**PQBD**, Scheme 1), a unique class of solid-state fluorescent dyes with red emission.

The design strategy for the **PQBD** dyes is formulated on the basis of the following considerations: (1) Selection of the phenanthro[9,10-*d*]imidazole moiety. It is known that phenanthro[9,10-*d*]imidazole dyes have large Stokes shifts (up to 100 nm),[4] which are favorable for solid-state emission by minimizing reabsorption and self-quenching.[5] In addition,

---

(1) (a) Brittenham, P. W.; Vittitow, M. P. Basic Research Needs for Solid-State Lighting. *Report of the Basic Energy Sciences Workshop on Solid-State Lighting*; May 22–24, 2006; Sandia Washington Program Office: Washington, DC, 2006. (b) Birks, J. B. *Photophysics of Aromatic Molecules*; Wiley: London, 1970. (c) Saragi, T. P. I.; Spehr, T.; Siebert, A.; Fuhrmann-Lieker, T.; Salbeck, J. *Chem. Rev.* **2007**, *107*, 1011. (d) Figueira-Duarte, T. M.; Müllen, K. *Chem. Rev.* **2011**, *111*, 7260.

(2) For some examples, see: (a) Yang, Y.; Su, X.; Carrollb, C. N.; Aprahamian, I. *Chem. Sci.* **2012**, *3*, 610. (b) Zhang, Z.; Xu, B.; Su, J.; Shen, L.; Xie, Y.; Tian, H. *Angew. Chem.* **2011**, *123*, 11858. (c) imizu, M. Sh.; Takeda, Y.; Higashi, M.; Hiyama, T. *Angew. Chem.* **2009**, *121*, 3707. (d) Wakamiya, A.; Mori, K.; Yamaguchi, S. *Angew. Chem., Int. Ed.* **2007**, *46*, 4273. (e) Kubota, Y.; Tanaka, S.; Funabiki, K.; Matsui, M. *Org. Lett.* **2012**, *14*, 4682. (f) Hong, Y.; Lama, J. W. Y.; Tang, B. Z. *Chem. Commun.* **2009**, 4332. (g) Mutai, T.; Tomoda, H.; Ohkawa, T.; Yabe, Y.; Araki, K. *Angew. Chem., Int. Ed.* **2008**, *47*, 9522.

(3) For some examples, see: (a) Qin, T.; Zhou, G.; Scheiber, H.; Bauer, R. E.; Baumgarten, M.; Anson, C. E.; List, E. J. W.; Müllen, K. *Angew. Chem., Int. Ed.* **2008**, *47*, 8292. (b) Fei, Z.; Kocher, N.; Mohrschladt, C. J.; Ihmels, H.; Stalke, D. *Angew. Chem., Int. Ed.* **2003**, *42*, 783. (c) Ozdemir, T.; Atilgan, S.; Kutuk, I.; Yildirim, L. T.; Tulek, A.; Bayindir, M.; Akkaya, E. U. *Org. Lett.* **2009**, *11*, 2105. (d) Kubota, Y.; Hara, H.; Tanaka, S.; Funabiki, K.; Matsui, M. *Org. Lett.* **2011**, *13*, 6544. (e) Li, D.; Zhang, H.; Wang, C.; Huang, S.; Guo, J.; Wang, Y. *J. Mater. Chem.* **2012**, *22*, 4319. (f) Gao, F.; Liao, Q.; Xu, Z. Z.; Yue, Y. H.; Wang, Q.; Zhang, H. L.; Fu, H. B. *Angew. Chem., Int. Ed.* **2010**, *49*, 732. (g) Lu, H.; Wang, Q.; Gai, L.; Li, Z.; Deng, Y.; Xiao, X.; Lai, G.; Shen, Z. *Chem.—Eur. J.* **2012**, *18*, 7852. (h) Zhou, Y.; Xiao, Y.; Li, D.; Fu, M.; Qian, X. *J. Org. Chem.* **2008**, *73*, 1571. (i) Kubota, Y.; Uehara, J.; Funabiki, K.; Ebihara, M.; Matsui, M. *Tetrahedron Lett.* **2010**, *51*, 6195.

(4) Lin, W.; Long, L.; Yuan, L.; Cao, Z.; Chen, B.; Tan, W. *Org. Lett.* **2008**, *10*, 5577.

(5) (a) Wang, Z.; Lu, P.; Chen, S.; Gao, Z.; Shen, F.; Zhang, W.; Xu, Y.; Kwok, H. S.; Ma, Y. *J. Mater. Chem.* **2011**, *21*, 5451. (b) Zhang, Y.; Lai, S. L.; Tong, Q. X.; Chan, M. Y.; Ng, T. W.; Wen, Z. C.; Zhang, G. Q.; Lee, S. T.; Kwonge, H. L.; Lee, C. S. *J. Mater. Chem.* **2011**, *21*, 8206.

10.1021/ol400605x

the phenanthro[9,10-*d*]imidazole moiety possesses an aromatic NH, which can be taken advantage of to coordinate with boron fluoride for enhancement of fluorescence quantum yields.[3d,6] Furthermore, the phenanthro[9,10-d]-imidazole moiety can function as an effective electron donor.[7] (2) Selection of the quinoline unit. The aromatic N atom of quinoline can be used as a ligand for the boron complex. Furthermore, in **PQBD**, the quinoline moiety bears a positive charge and thus can serve as an electron acceptor. Hence, with phenanthro[9,10-*d*]imidazole and quinoline moieties operating as electron donor and acceptor, respectively, **PQBD** may be considered as an effective donor (D)−acceptor (A) system, which is desirable for absorption and emission in the long wavelength. The D−A nature of **PQBD** is confirmed by density functional theory (DFT) studies. As shown in Figure S1 (Supporting Information), in **PQBD**, the π electrons of the HOMO molecular orbital are mainly located on the 1*H*-phenanthro-[9,10-*d*]imidazole moiety, whereas those of the LUMO are mostly positioned on the quinoline unit. To the best of our knowledge, boron difluoride-rigidified 1*H*-phenanthro-[9,10-*d*]imidazol-2-yl dye has not been previously used in the design of solid-state fluorescent dyes.

Scheme 1. Synthesis of Compounds **PQBD 1−6**

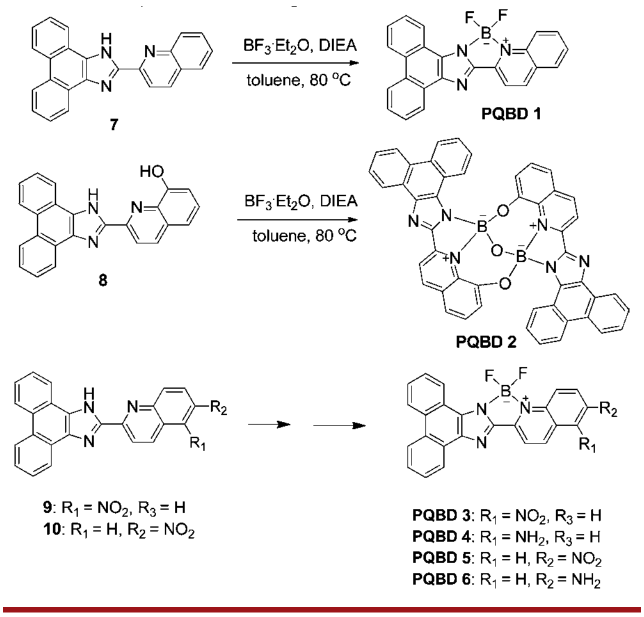

The key steps for the synthesis of new compounds **PQBD 1−6** are indicated in Scheme 1, and the full details are given in the Supporting Information (Schemes S1−7). Briefly, condensation of 1*H*-phenanthrene-9,10-dione with substituted quinoline-2-carbaldehyde in the presence of ammonium acetate gave the key intermediates **7**, **8**, **9**, and **10**, which were then treated with $BF_3 \cdot Et_2O$ in the presence of DIEA to provide the desired products **PQBD 1**, **2**, **3**, and **5**, respectively. In addition, nitro compound **PQBD 3** or **5** was reduced by $SnCl_2$ to afford amino compound **PQBD 4** or **6**, respectively. Interestingly, unlike **PQBD 1**, **3**, **4**, **5**, and **6**, **PQBD 2** exists as a dimer as confirmed by X-ray crystallography (vide infra). The formation of the dimer product with a B−O−B center is likely due to partial hydrolysis during the reaction.[8]

With the compounds **PQBD 1−6** in hand, we examined the absorption and emission spectra of these novel dyes in dichloromethane. The absorption and emission profiles are shown in Figure 1, and the photophysical data are summarized in Table S1 (Supporting Information). The major absorption peaks of **PQBD 1−6** are at 476, 472, 518, 468, 530, and 482 nm, respectively. The time-dependent density functional theory (TDDFT) studies show that the maximal absorption band is at around 525 nm (S0→S1, $f = 0.3524$) for **PQBD 1**, 539 nm (S0→S1, $f = 0.1918$) for **PQBD 3**, 514 nm (S0→S1, $f = 0.3491$) for **PQBD 4**, 565 nm (S0→S1, $f = 0.5364$) for **PQBD 5**, and 533 nm (S0→S1, $f = 0.3320$) for **PQBD 6**, respectively (Figure S3, Supporting Information). Thus, the trends in the calculated maximal absorption data are consistent with the experimental ones. Notably, the maximum absorption of **PQBD 3** and **5** is much more bathochromic than that of other compounds, attributed to the strong electron-withdrawing effect of the nitro group. In addition, **PQBD 5** with a nitro group at the *para* position exhibits a red-shift relative to **PQBD 3** with a nitro group at the *meta* position, highlighting the position effect of the substituent group. The same phenomenon was noted when compared **PQBD 6** with **PQBD 4**. Consistent with the trend observed in the absorption, the emission of **PQBD 3** and **5** display a marked red-shift in comparison to other dyes. These results are in good agreement with the calculated molecular orbitals and energy levels of **PQBD 1−6** (Figure S2, Supporting Information). The Stokes shifts of **PQBD 1−6** are up to 115 nm, which is significantly larger than those (less than 15 nm) of typical boron difluoride-rigidified dyes such as BODIPYs.[9] As shown in Figure S1 (Supporting Information), **PQBD 1−6** display the efficient electron transfer from the phenanthro[9,10-*d*]imidazole unit to the quinoline moiety. This effective intramolecular charge transfer process is consistent with the large Stokes shifts of the new dyes.[10]

PQBD exhibit very bright luminescence in dichloromethane (Figure 2). The relative fluorescence quantum yields of **PQBD 1−6** calculated using rhodamine 6G as a reference dye ($\Phi_F = 0.95$ in water) were estimated. As shown in Table S1 (Supporting Information), the fluorescence quantum yields of **PQBD 3** and **4** are significantly lower than those of other **PQBD** dyes. The

---

(6) Kubota, Y.; Tsuzuki, T.; Funabiki, K.; Ebihara, M.; Matsui, M. *Org. Lett.* **2010**, *12*, 4010.

(7) (a) Wang, J.; Lin, W.; Li, W. *Chem.—Eur. J.* **2012**, *18*, 13629. (b) Ooyama, Y.; Nagano, S.; Yoshida, K. *Tetrahedron* **2009**, *65*, 1467.

(8) Belcher, W. J.; Hodgson, M. C.; Sumida, K.; Torvisco, A.; Ruhlandt-Senge, K.; Ware, D. C.; Boyda, P. D. W.; Brothers, P. J. *Dalton Trans.* **2008**, 1602.

(9) (a) Ulrich, G.; Ziessel, R.; Harriman, A. *Angew. Chem., Int. Ed.* **2008**, *47*, 1184. (b) Loudet, A.; Burgess, K. *Chem. Rev.* **2007**, *107*, 4891.

(10) (a) Wang, B.; Liao, H.; Yeh, H.; Wu, W.; Chen, C. *J. Lumin.* **2005**, *113*, 321. (b) Cornelissen-Gude, C.; Rettig, W. *J. Phys. Chem. A* **1999**, *103*, 4371.

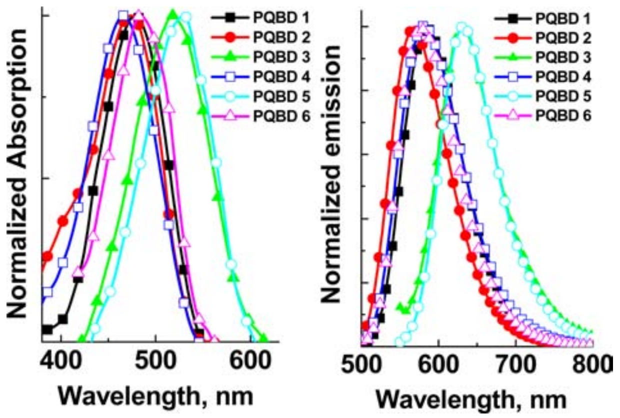

Figure 1. Normalized absorption and emission spectra of **PQBD 1**−**6** in dichloromethane.

fluorescence lifetimes (τ) of **PQBD 1**−**6** in CH_2Cl_2 were measured to be 4.89, 3.65, 2.67, 2.19, 2.18, and 2.96 ns, respectively (Figure S5, Supporting Information). The radiative ($k_f = \Phi_f \times \tau$) and nonradiative ($k_{nr} = (1 -\Phi_f)/\tau$) rate constants were also calculated (Table S1, Supporting Information). The relatively lower fluorescence quantum yields of **PQBD 3/5** when compared to **PQBD 4/6** can be attributed to the fluorescence quenching nature of the nitro group.

Generally, BODIPYs have no emission in the solid state partly due to small Stokes shifts. By sharp contrast, our new **PQBD** dyes have large Stokes shifts, which bodes well for the solid-state emission. Indeed, **PQBD 1**−**5** display intense red emission in the solid state (Figure 2). By contrast, **PQBD 6** shows solid-state yellow emission.

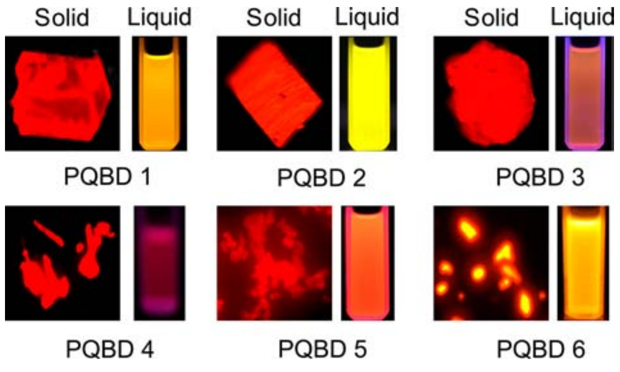

Figure 2. Photographs of **PQBD 1**−**6** in dichloromethane and in the solid state.

To gain the solid-state absorption and emission spectra, the films were prepared by evaporation of 500 μM dyes in dichloromethane onto a quartz plate. The absolute quantum yields of the dyes in powder were measured by Horiba Jobin Yvon-Edison Fluoromax-4 fluorescence spectrometer with a calibrated integrating sphere system. The absorption and emission spectra of **PQBD 1**−**6** in the solid state are shown in Figure S6 (Supporting Information) and Figure 3, respectively, and the photophysical data in the solid state are collected in Table S2 (Supporting Information). As anticipated, the new dyes in the solid state display a red-shift in the emission profiles relative to in dichloromethane. However, the emission wavelength of **PQBD 1**−**5** is much longer than that of **PQBD 6**, consistent with the above observation that **PQBD 1**−**5** and **PQBD 6** show red and yellow fluorescence in the solid state, respectively. The Stokes shifts of **PQBD 1**−**6** in the solid state are very large. For instance, **PQBD 4** bears a Stokes shift of 187 nm. The large Stokes shifts of the new family of dyes are consistent with the findings that they exhibit intense emission in the solid. It is known that long wavelength emission dyes tend to have quite low fluorescence quantum yields in solid. However, although **PQBD 1** and **2** have long wavelength emission in the red region, the fluorescence quantum yields of **PQBD 1** and **2** are still very high. In fact, the quantum yields of **PQBD 1** and **2** are at around 0.184 (Table S2, Supporting Information), which represent the highest values of solid-state red fluorescence boron difluoride-rigidified dyes. In particular, **PQBD 1** shows a chromaticity value, CIE (0.63, 0.36), which is close to the ideal red CIE (0.64, 0.34) (Figure S7, Supporting Information), indicating that **PQBD 1** with advantageous characters of a high fluorescence quantum yield and almost ideal red feature is promising for applications in optoelectronic materials.

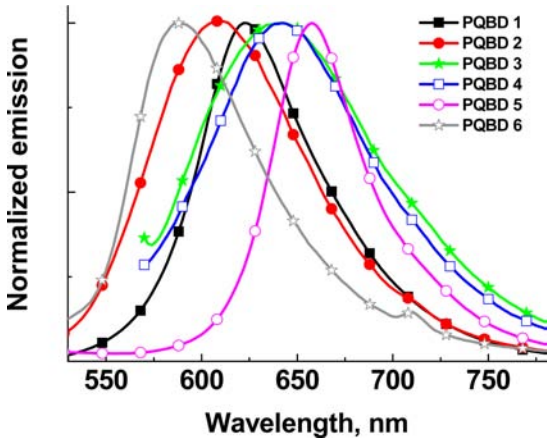

Figure 3. Fluorescence spectra of **PQBD 1**−**6** in the solid state (film). The excitation wavelength was 440, 470, 530, 520, 440, and 470 nm for **PQBD 1**, **PQBD 2**, **PQBD 3**, **PQBD 4**, **PQBD 5**, and **PQBD 6**, respectively.

To understand the spectroscopic properties of the new dyes in the solid state, their X-ray structures may be insightful; however, only single crystals of **PQBD 1** and **PQBD 2** suitable for X-ray structure analysis were obtained by the slow evaporation of CH_2Cl_2 or C_2H_5OH solutions

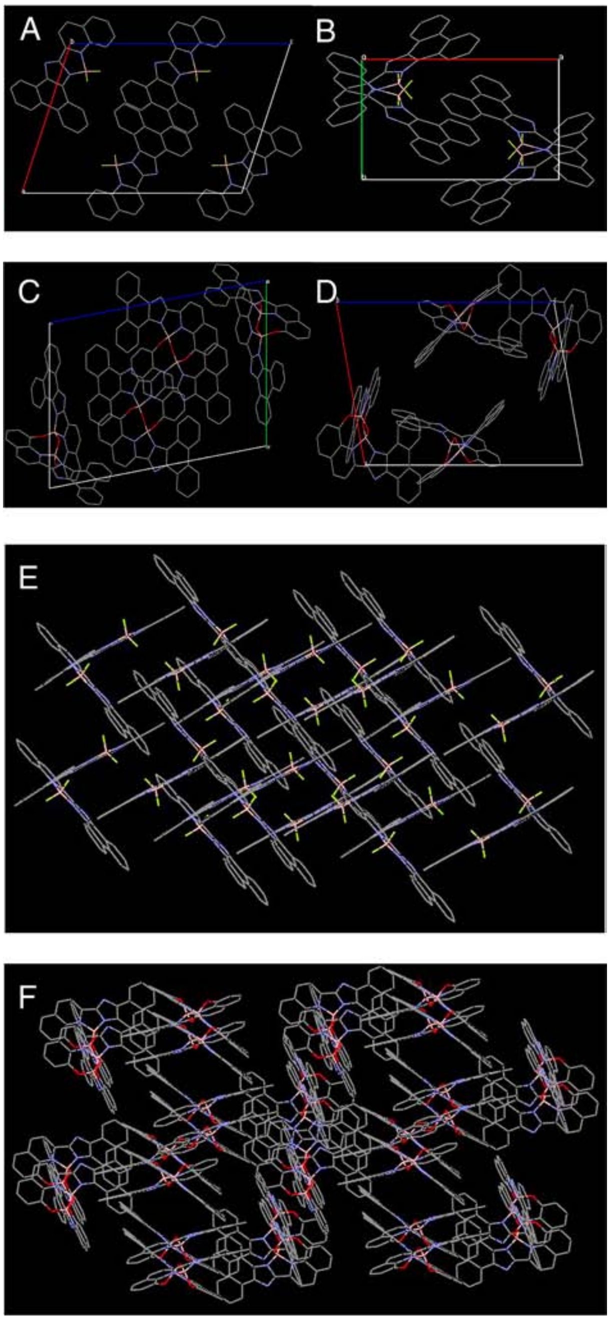

Figure 4. A part of a crystal-packing pattern of **PQBD 1** (A, along the *b* axis; B, along the *c* axis) and **PQBD 2** (C, along the *a* axis; D, along the *b* axis) that shows no stacking of the aromatic rings between the adjacent interlayered crystals. Packing diagrams view of **PQBD 1** (E) and **PQBD 2** (F).

at ambient temperature. The crystal structures unambiguously reveal the structural distinctions for these two dyes (Figures S8 and S9, Supporting Information). **PQBD 1** bears one F–B–F center, and the boron is coordinated in a tetrahedral geometry by two nitrogen and two fluorine atoms. The bond lengths of B–N are 1.641 and 1.616 Å, and those of B–F are 1.369 and 1.370 Å. **PQBD 1** is essentially planar. The boron atom only deviates from the plane of quinoline-phenanthro[9,10-*d*]imidazole at 0.88°, which is consistent with DFT optimized structure of **PQBD 1** (Figure S1, Supporting Information). In contrast, **PQBD 2** is a dimer with two O–B–O centers. The boron is coordinated in a tetrahedral geometry by two nitrogen and two oxygen atoms. The bond lengths of B–N are 1.550 and 1.641 Å, and those of B–O are 1.409 and 1.453 Å. The dihedral angle between one quinoline-phenanthro[9,10-*d*]-imidazole plane with another one is 103.6°. Thus, unlike planar **PQBD 1**, **PQBD 2** is highly twisted and far away from the coplanar framework. Despite that **PQBD 1** is planar, a careful examination of crystal lattice of **PQBD 1** reveals that no $\pi-\pi$ stacking interactions in a crystal lattice for head-to-head overlapping along the *b* axis and vertical overlapping along the *c* axis (Figure 4A,B,E, Figure S10, Supporting Information), which account for strong fluorescence in the solid state. In addition, the highly twisted structure of **PQBD 2** inhibits $\pi-\pi$ stacking, attributed to high solid-state emission (Figure 4C,D,F, Figure S11, Supporting Information).

In conclusion, a new family of boron difluoride-rigidified dyes, **PQBD**, with solid-state fluorescence has been designed and synthesized. The new series of the **PQBD** dyes are advantageous over typical boron difluoride-rigidified dyes such as BODIPYs in terms of large Stokes shift and red fluorescence in the solid state. We expect that the novel **PQBD** dyes will find valuable applications in development of fluorescent probes, organic luminescent displays, and light sources.

Acknowledgment. This research was supported by NSFC (20972044, 21172063), NCET (08-0175), and the Doctoral Fund of Chinese Ministry of Education (20100161110008)).

Supporting Information Available. Experimental procedures, absorption and emission spectra, DFT calculations, lifetime decay profiles, crystallographic data, CIF, and NMR spectra. This material is available free of charge via the Internet at http://pubs.acs.org.

The authors declare no competing financial interest.